

LOCKIN THERMOGRAPHY METHODS FOR THE NDT OF AIRCRAFT COMPONENTS

Th. Zweschper, A. Dillenz, G. Riegert, and G. Busse

University of Stuttgart - Institute of Polymer Testing and Polymer Science (IKP)
Department of Non-Destructive Testing
Pfaffenwaldring 32, D-70569 Stuttgart, Germany
e-mail address of lead author: zweschper@ikp.uni-stuttgart.de

1 Abstract

Lockin thermography is being used since several years for remote non-destructive testing. Optical excited lockin thermography (OLT) is based on propagation and reflection of thermal waves which are launched from the surface into the inspected component by absorption of intensity modulated radiation. Phase angle images obtained by superposition of the initial thermal wave and its reflection display hidden thermal structures down to a certain depth below the surface. Defects are found by comparing the observed features with expected features provided by theory or by an intact reference sample.

Defect detection is much easier if a mechanism is involved where a defect responds selectively so that the image contains only the defect and not the confusing background of intact features. Elastic waves sent into the component propagate inside the sample until they are converted into heat. A defect causes locally enhanced losses and consequently selective heating. Therefore modulation of the elastic wave amplitude results in periodical heat generation so that the defect is turned into a local thermal wave transmitter. Its emission is detected via the temperature modulation at the surface which is analysed by lockin thermography tuned to the frequency of amplitude modulation. The amplitude image displays the efficiency of local mechanical losses, so it shows the imaginary part of elastic properties. Though the technique is related to ultrasonic inspection, the ultrasonic transducer is attached at a fixed spot from where the acoustic waves are launched into the whole volume where they are reflected several times until they disappear preferably in a defect and generate heat. These high frequencies are very efficient in heating since many hysteresis cycles are performed per second. Corresponding measurements are being performed using burst excitation providing depth resolved phase angle images.

In this paper we present measurements performed on various kinds of aerospace structures (both metal and non-metal) containing typical defects. The obtained phase angle images reveal areas of hidden corrosion, cracks in rows of rivets, disbonds, impacts, and

delaminations. In all these cases the intact structure was suppressed since it heats up much less in the elastic wave field. We present examples which are relevant e.g. for maintenance and inspection of aging aircraft.

2 Introduction

Reliable inspection techniques are required for the maintenance of safety relevant structures (e.g. aerospace equipment and vehicles) where one needs to detect defect areas early enough to prevent catastrophic failure. As many structures consist of carbon fiber reinforced plastics (CFRP), the rapid and remote identification of delaminations, impact damages, ruptures, and cracks is a topic of major concern. Therefore a method is required that is applicable during inspection procedures to monitor the integrity of such structures.

2.1 External excitation: Optical Lockin Thermography (OLT)

Thermal waves [1] have been used very early for remote monitoring of thermal features, e.g. cracks, delaminations [2], and other kinds of boundaries. After the advantage of signal phase had been discovered [3-5], phase angle imaging using photothermal techniques [6] became a powerful tool for imaging of hidden structures due to the enhanced depth range and its independence on optical [7] or infrared surface patterns.

As the thermal diffusion length is the important parameter for depth range [8], it turned out very soon that imaging of features deep underneath the surface requires very low modulation frequencies and a correspondingly long time to obtain a photothermal image. Unfortunately many industrial questions are related to samples with defects at about a millimeter depth. An image obtained pixel after pixel at a modulation frequency in the 1 Hz range could easily require several hours.

One approach allowing for a reduction of inspection time is lockin thermography where the low frequency thermal wave is generated simultaneously on the whole surface of the inspected component and monitored everywhere several times per modulation cycle in order to obtain an image of amplitude and phase of temperature modulation [9-12]. In this case the inspection time is given by a few modulation cycles. As one can image square meters of airplanes within a few minutes [13], one has a powerful method for fast inspection of safety relevant structures with a depth range of several millimeters in CFRP.

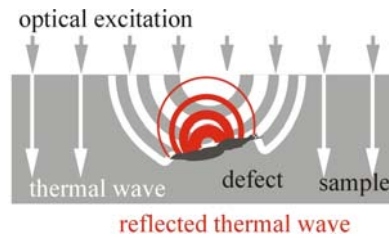


Figure 1. Principle of lockin thermography with optical excitation (OLT).

Therefore both defects and intact structures are imaged at the same time. Defects can be revealed only by comparing the observed features with expected patterns provided by theory, by reference samples, or by design drawings. Even for an experienced inspector it is difficult to distinguish defect areas from these thermal features.

2.2 Internal excitation : Ultrasound Lockin Thermography (ULT)

Further investigations aimed at a method where a defect responds selectively so that the image would display only the defect and not the confusing background of the intact structure. Defects differ from their surroundings by their mechanical weakness. They may cause stress concentrations, and under periodical load there may be hysteresis effects or friction in cracks and delaminations. As defects may be areas where mechanical damping is enhanced, the ultrasound is converted into heat mainly in defects [14, 15]. Modulation of the elastic wave amplitude results in periodical heat generation so that the defect is turned into a local thermal wave transmitter (Figure 2). Its emission is detected via the temperature modulation at the surface which is analysed by lockin thermography tuned to the frequency of amplitude modulation [16]. The ultrasonic transducer is attached at a fixed spot from where the acoustic waves are launched into the whole volume where they are reflected several times until they disappear preferably in a defect and generate heat. These high frequencies are very efficient in heating since many hysteresis cycles are performed per second.

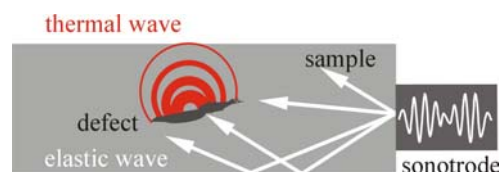


Figure 2. Principle of lockin thermography with ultrasonic excitation (ULT).

2.3 Internal excitation :Ultrasound Burst Phase Thermography (UBP)

Another established method is the use of short sonic bursts for sample excitation [17] (Figure 3). The spectral components of that signal and the following cooling down period provide information about defects in almost the same way as Lockin technique but with reduced measuring duration. As the characteristic defect signal is contained in a limited spectral range while the noise typically is distributed over the whole spectrum, one can reduce noise as well. That kind of evaluation technique using Fourier or Wavelet transformations is also applicable to flash-light excited thermography [18-20]. The signal to noise ratio of ULT and UBP images (and hence defect detectability) is significantly better than just one temperature snapshot image in a sequence [21, 22].

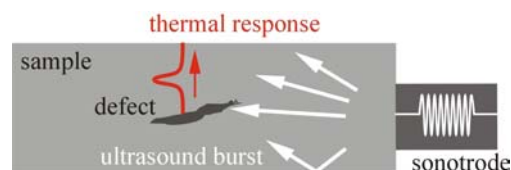


Figure 3. Principle of ultrasound burst thermography (UBP).

The following example confirms that high frequencies probe only near-surface areas while low frequencies with their larger depth range provide information about defects deeper inside the component. Thus depth resolved mapping of defects can be performed with only one measurement.

For this demonstration we manufactured a sample with four delaminations in various depths between 0.2 mm and 2.2 mm. After an ultrasonic burst of 100 ms duration had been injected the resulting temperature sequence was evaluated at various frequencies. In the phase image at 3 Hz (Figure 4a) only the defect near the surface causes a change in the phase angle. At 1 Hz (Figure 4b) already three delaminations in depths from 0.2 mm to 1.5 mm become visible. At 0.5 Hz (Figure 4c) all defects appear. At an even lower frequency (0.1 Hz, see Figure 4d) the image contrast is reduced due to lateral diffusion effects.

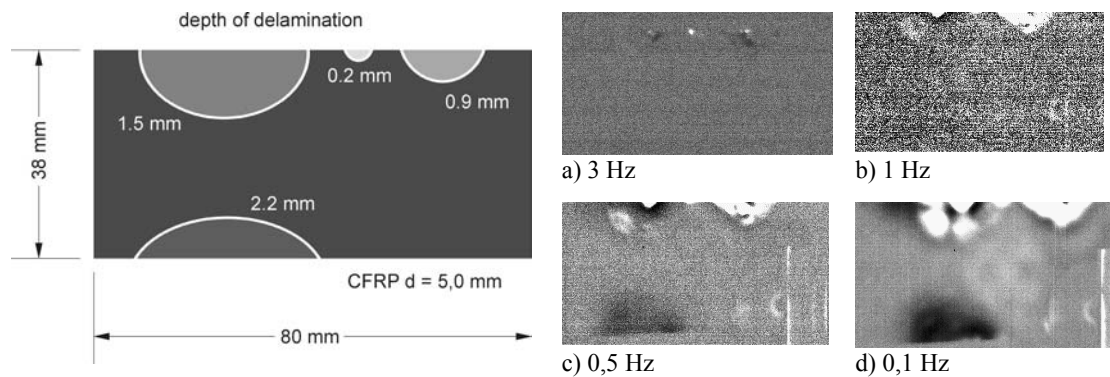


Figure 4. UBP images of a CFRP sample with delaminations in different depths. Excitation: 1 kW, ultrasonic frequency 20 kHz, burst duration: 100 ms.

3 Experimental arrangement

For our experiments we used a CEDIP infrared focal plane array camera (Jade II). The 320 x 240 detector array responds to radiation in the 3-5 μm spectral band at a frame rate up to 200 Hz. The experimental configuration for OLT is illustrated on the left side in Figure 5. A lockin module and a signal generator controlled the light source (generating the thermal waves) which is synchronised to the recording process of thermal images. We use up to six halogen lamps each with an electrical input power of 1 kW. Up to 12 lamps can be used allowing for an inspection area of several m^2 . The phase angle between the sinusoidal illumination of the sample surface and the local thermal wave response (affected by reflection from defects) is colour coded and visualized on the monitor as a phase angle image of the inspected surface area.

Figure 5 (right) displays the corresponding experimental ULT arrangement. The acoustic or ultrasonic transducer is attached to the component which is monitored by a lockin thermography system tuned to the low frequency of amplitude modulation. The elastic wave frequency was typically around 20 kHz while the amplitude modulation frequency was usually below 1 Hz. The acoustic energy provided by the source was in most experiments several hundred Watts. Duration of a measurement was typically 3 minutes.

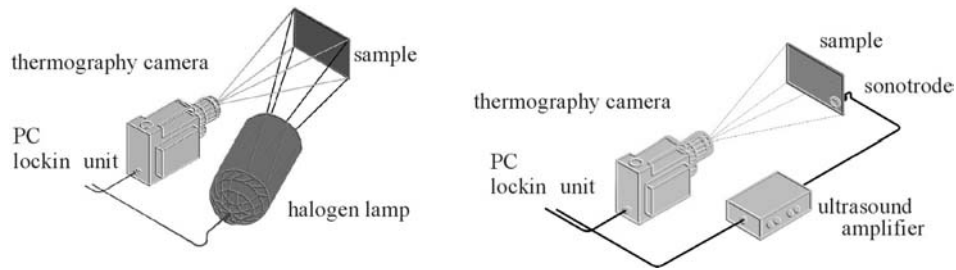


Figure 5. Experimental set-up of optical (OLT, left) and ultrasound excited lockin thermography (ULT, right).

Due to the significance of non-destructive inspection for safety-relevant structures we applied these techniques (OLT, ULT, and UBP) not only to various CFRP components but also to metal and ceramic aircraft structures. The results obtained by this defect-selective technique will be described below.

4 Results

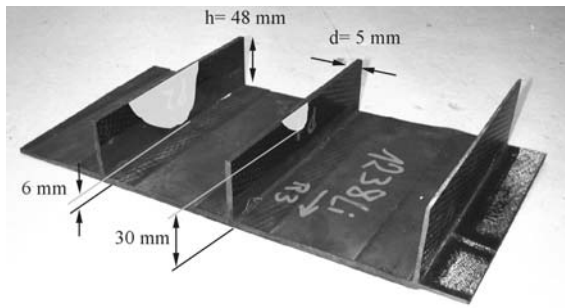
4.1 Non-metals

4.1.1 Ruptures, delaminations, and cracks in CFRP stringer structures

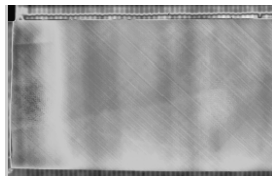
Stringers are used if stiffness needs to be enhanced along a certain direction. Consequently, stringer disbond caused e.g. by excessive loading results in a loss of structural stiffness. Therefore one is highly interested to detect such defects early enough to prevent failure.

Ruptures of stringers in aerospace components are a serious problem because this kind of damage is almost invisible from the outer surface of an aircraft for most non-destructive testing methods, since stringers are hidden behind a panel. The access from inside the aircraft is difficult and time consuming.

The CFRP structure to be inspected had ruptures in its stringers as shown schematically in Figure 6a. The damage was covered by a CFRP skin with a thickness of more than 6 mm. While stringer delaminations can be detected with Optical Lockin Thermography [13], the depth range of optically generated thermal waves is not sufficient to reveal hidden stringer ruptures (Figure 6b). Ultrasound Lockin Thermography (Figure 6c and 6d) and Ultrasound Burst Phase image (Figure 6e) can reveal the rupture in the left stringer clearly. The damage in the right stringer is too far from the surface (30 mm), therefore it remains undetected even with sonic excitation.



a) CFRP stringer structure
 thickness of skin: 6 mm.
 Laminated stringer (thickness 5 mm, height 48 mm).
 Ruptures are marked white.



b) Optical Lockin
 Thermography Phase
 image at 0.01 Hz, 200
 seconds acquisition time



c) Ultrasound Lockin
 Amplitude image at 0.01
 Hz, 400 W, and 100
 seconds acquisition time



d) Ultrasound Lockin Phase
 image at 0.01 Hz, 400 W,
 and 100 seconds
 acquisition time



e) Ultrasound Burst Phase
 image at 0,0485 Hz,
 burst length 5s, 400 W

Figure 6. Comparison of different phase images of ruptures in an aerospace component

Another example is a flap (Figure 7) where the results of OLT and ULT are compared. While OLT displays the whole structure where the small effect of the defect readily escapes attention, a small white spot in the ULT image indicates a crack and a delamination in the stringer underneath the intact CFRP-skin.

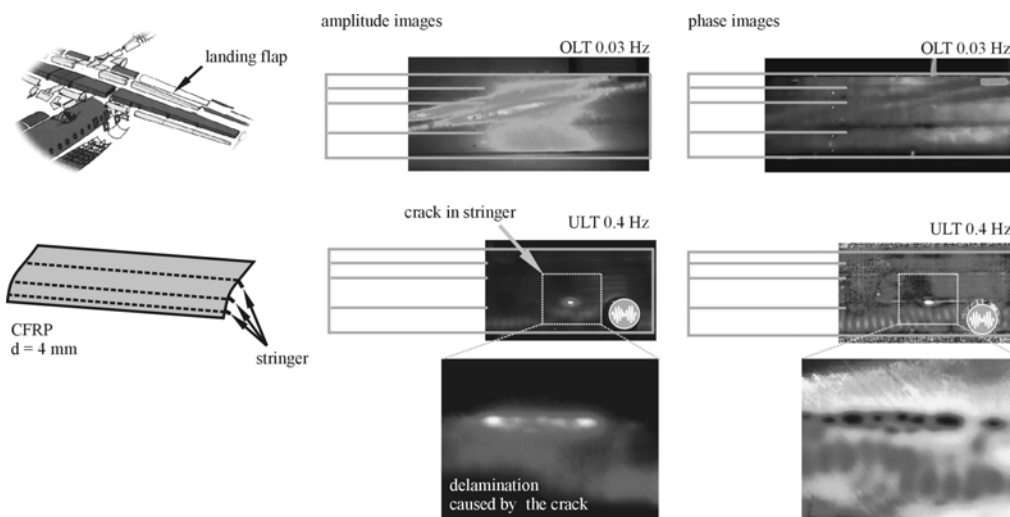


Figure 7. Comparison of OLT and ULT images of a delamination caused by a crack

Another example is the component investigated previously [23]. The photograph of the rear surface displays the structure that needs to be inspected with access only from the flat front surface. It is composed of a CFRP skin and T-shaped stringers bonded to it while the lighter rectangular areas are glass fiber reinforced polymer (GFRP) wedges attached to the structure to perform tests under load. With OLT performed on the front surface the intact structure (including the GFRP area) is revealed where the disbond appears as an interruption of the straight lines which indicate the bonded stringers. The ULT phase image shows only the area where the disbond starts since only there the components can rub against each other in the ultrasound field. Surprisingly, there is an additional small spot which is not due to disbond but rather to a crack in the perfectly bonded stringer so that the heat modulation generated by friction can propagate as a thermal wave across the bond into the front of the skin over a cm-distance.

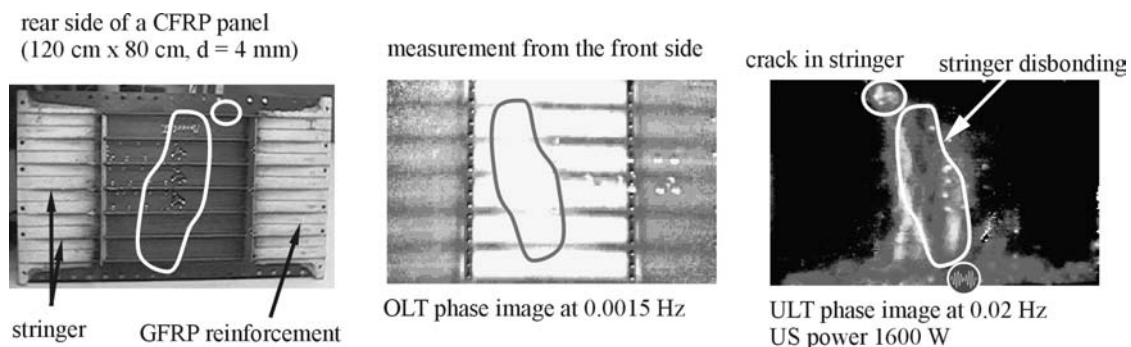


Figure 8. Stringer disbonding and cracks in an aircraft panel. Left: Optical image of rear side. Results of OLT (middle) and ULT (right) obtained on flat front surface.

4.1.2 Damage detection using small piezo-ceramic actuators

From previous investigations it is known that soft materials could be damaged by injecting elastic waves with high energy [24]. An alternative approach is the use of many small distributed piezo-ceramic actuators to generate an elastic wave field in the inspected component. This results in a reduction of mechanical and thermal load. Here we examined a thin carbon fiber plate with seven impact damages. Three piezo-ceramic actuators were bonded to the sample to generate a wave field at a frequency of 8 kHz with 200 W during 1 second. Some milliseconds after the excitation burst, the best thermal contrast for defect detection is achieved (Figure 9a). However, there is only a small change in temperature at the damaged regions of the sample. The amplitude image calculated with a Fourier transform at

0.24 Hz is an improvement in terms of signal to noise ratio (Figure 9b). The defects are displayed with better contrast, but friction between sample and actuators still causes thermal fringes around the actuators. This effect is much reduced in the phase image derived from the same sequence (Figure 9c), where inhomogeneity of temperature variations are eliminated.

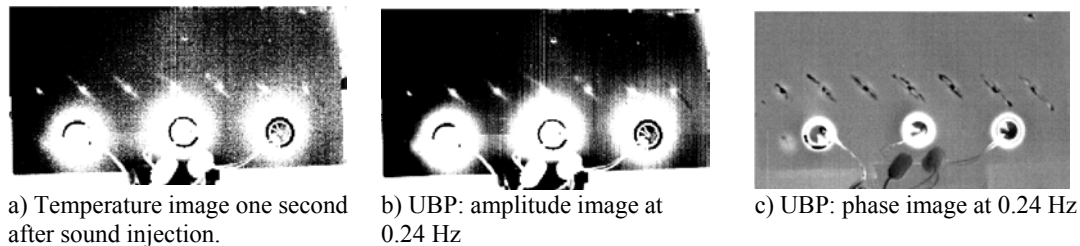


Figure 9. UBP: amplitude and phase image of seven impacts in CFRP ($d = 2$ mm)

4.1.3 Sandwich structures

Honeycomb structures are being used in aerospace applications due to their low weight and high stiffness. The critical area of such a component is where the skin is bonded to the structure underneath. Condensation of water can affect the quality of bonding which might result in a loss of adhesion and finally in a local loss of stiffness. That is why the reliable detection of water underneath a perfect outer skin is important for maintenance inspection. Such an example is presented in Figure 10 where parts of the honeycomb structure had been filled with water with an injection needle from the rear surface while inspection was performed from the front surface.

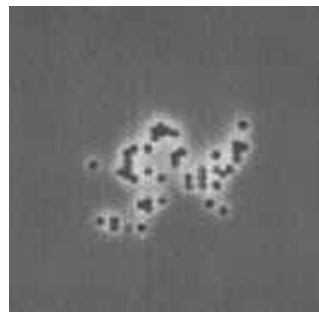


Figure 10. Water in a honeycomb structure. OLT amplitude (left) and phase signature (right) at a lockin frequency of 0.1 Hz.

4.2 Metals

Ultrasound activated thermography is one of the few techniques that can detect cracks independently of their orientation: multiple reflections of the elastic wave inside the component eliminate its directionality. Therefore all cracks will be “hit” by a suitably directed ultrasonic wave after some time and thus be reliably recognized.

4.3 Turbine blades

Stress cracks in turbine blades caused by extreme thermal loading are a serious problem for manufacturers of jet engines. The example (Figure 11) shows crack detection using ultrasound burst phase thermography. These cracks propagating from the outlets of the cooling channels light up after a short ultrasound burst (typically a few hundred milliseconds). The phase evaluation of the recorded temperature images (middle) provides a defect selective image of the cracks that can be combined with the primary image (left) in order to locate the defect (right).

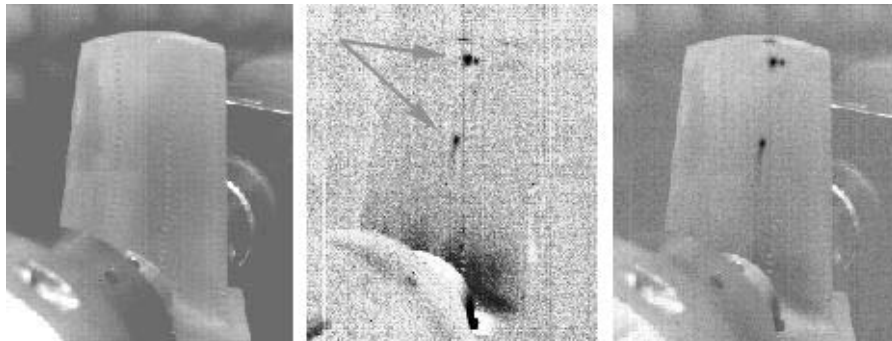


Figure 11. Crack detection in a ceramic coated turbine blade. Thermal image at 3-5 μm (left), ultrasound burst phase image at 0.1 Hz (middle), and the combined image (right).

4.4 Rivets

The detection of a crack along a row of rivets as an example for the maintenance and inspection of safety relevant structures is shown in Figure 12. The crack length had been known from eddy current inspection (Figure 12a).

The amplitude image taken at 0.11 Hz using OLT (Figure 12b) displays the influence of the non-uniform intensity distribution. As the phase image (Figure 12c) is insensitive such perturbations, it shows essentially the thermal features between the surface and a depth of about twice the thermal diffusion length μ [3-5]. One can recognize clearly the reinforcement

of the aluminium plate on the right and the seemingly intact riveting. No damage and no crack could be detected.

Using ultrasonic excitation, however, a bright area was found with a significantly larger extension (Figure 12d). These rivets provide a reduced compressive stress so that the integrity of the riveting is no longer sure. The ULT measurement revealed that the damaged area is larger than expected from the eddy current results. To detect the crack only and to reaffirm the eddy current results, all rivets were removed and an amplitude (Figure 12e) and a phase image (Figure 12f) were taken again with ULT. As there was no more any rubbing contact to the rivets or the rib, only the tip of the crack caused hysteresis losses whose locations are identical with those found with eddy current measurement. The hot spot on the left was caused by the rubbing contact between rib and plate. This example shows how efficiently ULT can be applied for the selective imaging of fatigue cracks.

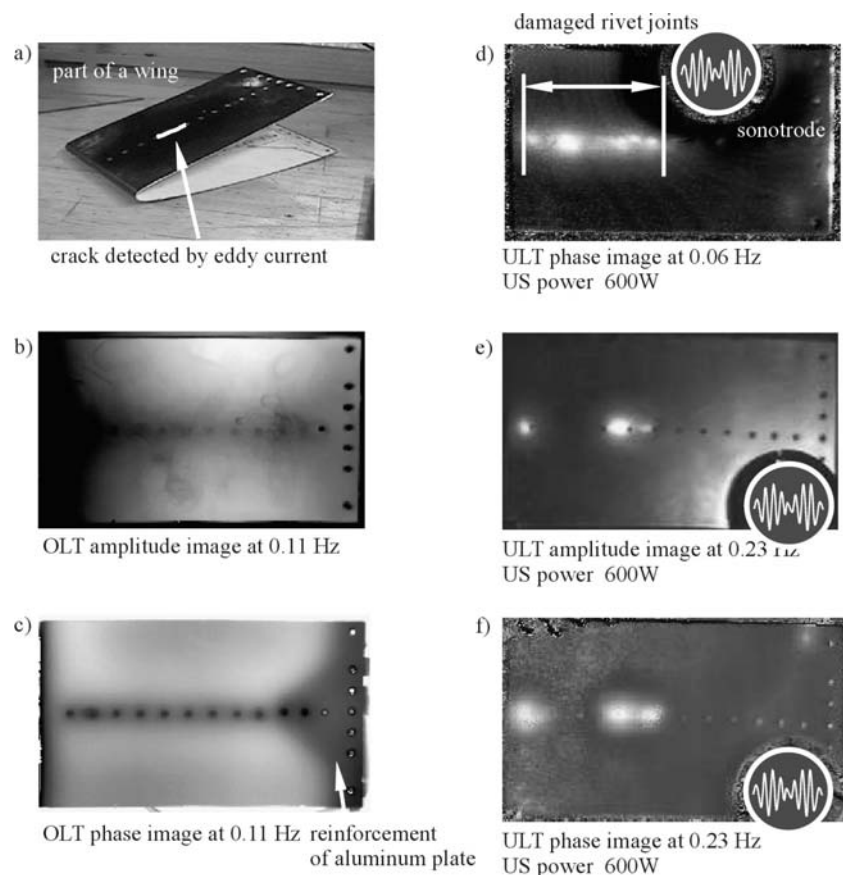


Figure 12. Detection of damaged rivet joints caused by cracks in an aluminium aircraft skin.

4.5 Ceramic structures

4.5.1 C/CSiC

Re-entry vehicles undergo rapid temperature changes where the material needs to withstand high temperatures. The same requirement holds for break disks of high speed trains: In both cases the mechanical properties may not be affected by sudden heating. Therefore it is essential to detect material inhomogeneities possibly caused by the production process of carbon fiber reinforced silicon carbide (C/C-SiC). This process includes immersion of the heated carbon fiber network into liquid silicon which diffuses into the material where it reacts to SiC which is an extremely hard material. If the diffusion speed is not well tuned, the material may be inhomogeneous due to concentration gradients of Si. This may result in boundaries and potentially also in cracks which are a source of trouble when the material is used. Such material had been inspected both with ULT and OLT (Figure 13). With optical excitation (OLT) where the generated thermal waves start at the surface and are reflected back to it at internal material gradients or boundaries (see Figure 1), one finds a broad area where the thermal properties are different. With ULT one sees only lines starting at the edge of this area. They might be correlated with cracks caused by high gradients when the material cooled down. Here one needs to know what the structures really mean which are found by application of advanced NDE methods. It is not enough to see that “there is something”. However, one must keep in mind that such questions still exist even in X-ray techniques though they are around since many decades. To interpret these features one needs to learn interpretation art least empirically by correlating NDE results with those of destructive testing (e.g. optical inspection of material slices cut along such NDE-patterns).

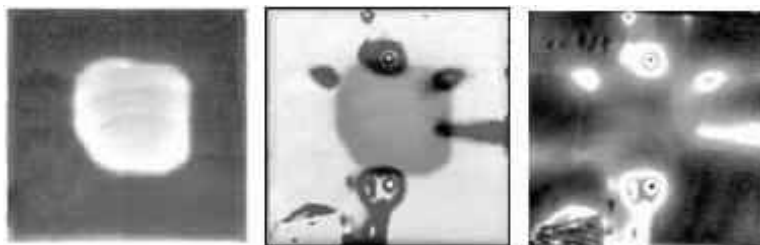


Figure 13. Phase images of a C/C-SiC sample at 0.03 Hz. Optical lockin thermography (left), ultrasound lockin thermography (right), and the combined image of both (middle).

While this was only a sample with a size of about 100 square inches, there is an obvious need to inspect real components made of this material. The geometry of these components may

differ significantly from a flat plate, and they may be much larger. We found that structural integrity can be monitored (Figure 14) under such conditions in a very fast and reliable way.

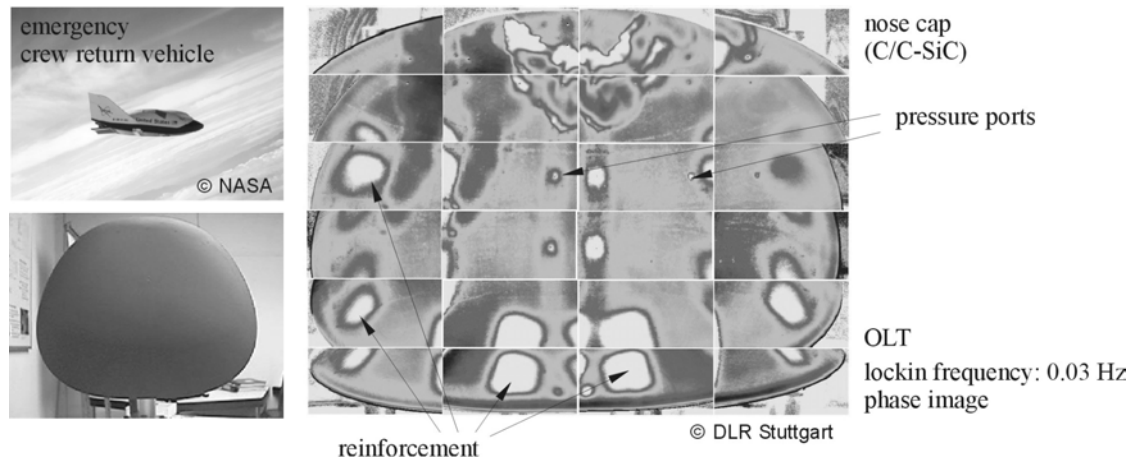


Figure 14. Phase image of a C/C-SiC nose cap of an emergency crew return vehicle.

5 Conclusion

Phase thermography (Lock-in or Burst) has some advantages as compared to conventional pulse thermography: sensitivity variations within the detector array as well as optical sample characteristics are suppressed. Furthermore the signal to noise ratio is improved significantly. Compared to OLT, using the ULT / UBP methods in CFRP defects can be detected up to a depth of 12 mm. Using UBP the probability of defect identification is thus improved at a reduced measuring time. The measurements presented in this paper show that even larger components can be examined with this technique.

However, the high excitation power contained in short pulses or bursts could possibly cause damage of the inspected structure. Standing waves can occur if the frequency applied to the sample fits to a mechanical resonance. Due to hysteretic losses in the strain maximum, these standing elastic waves can appear as temperature patterns which can cause misinterpretations. To eliminate standing wave patterns and to reduce the high excitation power the application of small distributed piezo-ceramic actuators was investigated. Good results were found for relatively small samples. However, the excitation efficiency must be improved to make this technique applicable to non-destructive testing of large structures.

No technique offers a solution to all problems. Within the field of non-destructive testing and evaluation a combination of different techniques may be required. Nevertheless the lock-in thermography methods with their capability of producing rapid scans across large areas and

defect selective imaging (in case of ULT and UBP) may provide a solution to the problem of quantitative in-service and manufacturing process inspection not only of commercial aircraft components.

6 Acknowledgements

The authors are grateful to DLR (Stuttgart, Germany) and MTU (Munich, Germany) for cooperation and providing samples. We also would like to thank Airbus (Bremen, Germany), Eurocopter (Ottobrunn, Germany), Dornier (Manching, Germany), WIWEB, and Luftwaffenwerft 13 (Erding, Germany) for providing aircraft structures. Financial support of the State of Baden-Wuerttemberg for the development of defect-selective imaging techniques is highly appreciated as well.

7 References

- [1] Fourier J.: Théorie du mouvement de la chaleur dans les corps solides, 1re Partie. In: Mémoires de l'Académie des Sciences 4 (1824) pp.185-555.
- [2] Wong Y. H.; Thomas R. L.; Pouch J. J.: Subsurface structures of solids by scanning photoacoustic microscopy. In: Appl. Phys. Lett. 35 5 (1979) pp. 368-369.
- [3] Busse G.: Optoacoustic phase angle measurement for probing a metal. In: Appl. Phys. Lett. Vol. 35 (1979) pp. 759-760.
- [4] Thomas R. L.; Pouch J. J.; Wong Y. H.; Favro L. D.; Kuo P. K.; Rosencwaig A.: Subsurface flaw detection in metals by photoacoustic microscopy. In: J. Appl. Phys. Vol. 51 (1980): pp. 1152-1156.
- [5] Lehto A.; Jaarinen J.; Tiusanen T.; Jokinen M.; Luukkala M.: Amplitude and phase in thermal wave imaging. In: Electr. Lett. Vol. 17 (1981): pp. 364-365.
- [6] Nordal, P.-E.; Kanstad S.O.: Photothermal radiometry. In: Physica Scripta Vol. 20 (1979): pp. 659-662.
- [7] Rosencwaig A.; Busse G.: High resolution photoacoustic thermal wave microscopy. In: Appl. Phys. Lett. Vol. 36 (1980): pp. 725-727.
- [8] Rosencwaig A.: Photoacoustic microscopy. In: American Lab. 11 (1979) pp. 39-49.
- [9] Carlomagno G. M.; Berardi P. G.: Unsteady thermotopography in non-destructive testing. In: Proc. 3rd Biannual Exchange, St. Louis/USA, 24.-26. August 1976, pp. 33-39.
- [10] Beaudoin J. L.; Merienne E.; Danjoux R.; Egee M.: Numerical system for infrared scanners and application to the subsurface control of materials by photothermal radiometry. In: Infrared Technology and Applications, SPIE Vol. 590 (1985) p. 287.
- [11] Kuo, P.K.; Feng Z. J.; Ahmed T.; Favro L. D.; Thomas R. L.; Hartikainen J.: Parallel thermal wave imaging using a vector lock-in video technique. In: Photoacoustic and

- Photothermal Phenomena, ed. P. Hess and J. Pelzl. Heidelberg: Springer-Verlag. (1987) pp. 415-418.
- [12] Busse, G., Wu D. and Karpen W.: Thermal wave imaging with phase sensitive modulated thermography. In: J. Appl. Phys. Vol. 71 (1992): pp. 3962-3965.
- [13] Wu, D.; Salerno A.; Malter U.; Aoki R.; Kochendörfer R.; Kächele P. K.; Woithe K.; Pfister K.; Busse G.: Inspection of aircraft structural components using lockin-thermography. In: Quantitative infrared thermography, QIRT 96, Stuttgart, ed. D. Balageas, G. Busse, and G. M. Carlomagno. Pisa: Edizione ETS (1997): pp. 251-256. ISBN 88 - 467 - 0089 - 9
- [14] Mignogna R. B.; Green R. E., Jr.; Duke; Henneke E. G.; Reifsnider K.L.: Thermographic investigations of high-power ultrasonic heating in materials. In: Ultrasonics 7 (1981) pp. 159-163.
- [15] Stärk F.: Temperature measurements on cyclically loaded materials. In: Werkstofftechnik 13, Verlag Chemie GmbH, Weinheim (1982) pp. 333-338.
- [16] Rantala J.; Wu D.; Busse G.: Amplitude Modulated Lock-In Vibrothermography for NDE of Polymers and Composites. In: Research in Nondestructive Evaluation, Vol. 7 (1996) pp. 215-218.
- [17] Patent DE 100 59 854.4
- [18] Maldague, X.; Marinetti, S.: Pulse Phase Infrared Thermography, J. Appl. Phys, 79 [5]: 2694-2698, 1 March 1996.
- [19] Galmiche, F.; Vallerand, S.; Maldague X.: Pulsed Phase Thermography with the Wavelet Transform, Review of Progress in Quantitative NDE, D.O. Thompson et D.E. Chimenti eds, Am. Institute of Physics, 19A: S. 609-615, (Montréal Juli 1999), 2000.
- [20] Maldague, X.; Marinetti, S.; Busse, G.; Couturier, J.-P.: Possible applications of pulse phase thermography. Progress in Natural Science. Supplement to Vol. 6, December 1996, S. 80-82
- [21] L. D. Favro, Xiaoyan Han, Zhong Ouyang, Gang Sun, Hua Sui, and R. L. Thomas, Infrared imaging of defects heated by a sonic pulse, Rev. Sci. Inst. 71, 6, 2000, S. 2418-2421.
- [22] R. L. Thomas, L.D. Favro, P. K. Kuo, T. Ahmed, Xiaoyan Han, Li Wang, Xun Wang and S.M. Shepard, Pulse-Echo Thermal-Wave Imaging for Non-Destructive Evaluation, Proc. 15th International Congress on Acoustics, Trondheim, Norway, June 26-30, 1995, S. 433-436.
- [23] Salerno, A.; Dillenz, A.; Wu, D.; Rantala, J.; Busse, G.: Progress in ultrasonic lockin thermography. Quantitative infrared thermography, QIRT 98. Akademickie Centrum Graficzno-Marketingowe Lodart S.A., Lodz 1998, S. 154-160. ISBN 83-87202-88-6
- [24] Dillenz, D.; Zweschper, Th.; Busse, G.: Progress in ultrasound phase angle thermography, Thermosense 2001, Orlando, USA.